Sediment Problems: Strategies for Monitoring, Prediction and Control (Proceedings of the Yokohama Symposium, July 1993). IAHS Publ. no. 217, 1993.

A method for estimating soil erosion caused by surface runoff using sloping lysimeters

K. BANZAI
National Institute of Agro-Environmental Sciences, Kannondai 3-1-1, Tsukuba, Ibaraki 305, Japan

Y. HAYASE
National Research Institute of Agricultural Engineering, Kannondai 2-1-2, Tsukuba, Ibaraki 305, Japan

Abstract A new soil loss equation was developed using soil loss data obtained from lysimeter experiments. Relationships between the dimensionless tractive force and the dimensionless sediment transport rate could be expressed by a linear regression on a log-log scale for two types soil, a sandy soil and a volcanic ash soil. By introducing the equation of motion in a kinematic wave model, a simple power function was obtained including variables of slope angle and rainfall rate which were measured in situ. This hydrological soil loss equation fitted well the experimental soil loss data which were associated with natural and simulated rainfall.

INTRODUCTION

Soil transport in the water erosion process by tractive force of the surface water flow is a complex phenomenon caused by the iteration between the friction force, flow velocity and soil properties at the boundary between the stream bed and water flow. Sediment transport in the soil erosion process in farmland is different from the sediment transport occurring due to a comparatively deep stream in a channel bed, because the sediment transport in farmland is caused by shallow laminar flow 1 to 10 mm in depth. Various hydraulic soil transport models have been designed by Iwagaki & Tsuchiya (1957), Yalin (1963), Kilinic (1973), Komura (1976), Finkner *et al.* (1989) and others for the sediment transport related to the tractive force of laminar flow or stream flow of shallow depth. However, these equations are rather complex and the determination of the coefficients is not always easy.

In this paper, we introduced a dimensionless tractive force and dimensionless sediment transport rate which were expressed as a power regression equation similar to that of Kalinske (Rouse, 1949). This dimensionless equation was transformed into an equation for the estimation of sediment transport using the equation of a Kinematic wave model. Data of surface water flow and sediment transport rate were collected based on studies using sloping lysimeters that were carried out of the National Research Institute of Agricultural Engineering, Japan.

EQUIPMENT AND MEASUREMENTS

Lysimeters

The lysimeters studied were 10 m long, 2.5 m wide and 2.0 m deep as shown in Fig. 1. The slope angles of the lysimeters were fixed at 5°, 7°, 10° and 15° in gradient. Two types of soils, volcanic ash soil and sandy soil, were filled up in the lysimeters and their surfaces remained bare.

A rain simulator with ten thousand plastic nozzles 10 x 10 m in area was set at a 4 m height at above lysimeters and moved on two parallel rail roads. The rain simulator covered four lysimeters at the same time. Intensities of rainfall could be adjusted in the range between 10 and 150 mm/h. Energy of the rain falling from the simulator was estimated at about 28 J/(m^2-mm).

Surface runoff

Surface runoff and sediment from each lysimeter were collected in a sedimentation ditch with a constant water depth and the amount of water which overflowed from the ditch was measured using a tipping bucket through a tube. Tipping electric pulses were counted with a recorder.

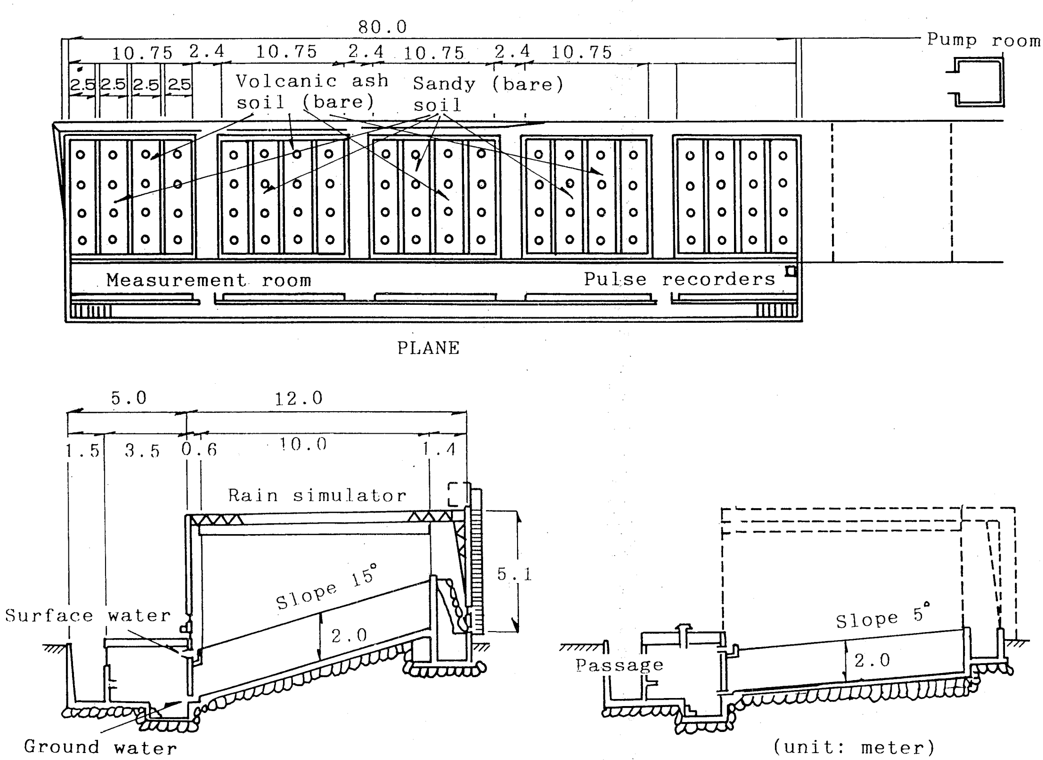

Fig. 1 Ground plane and sections of lysimeters.

Water depth of the surface water flow was measured with a point gauge at about 20 points along a line running in the right direction to the flow near the end of the sloping lysimeter (seven degrees) so as to calculate the mean depth (Banzai *et al.*, 1988).

Eroded sediment

Eroded sediment produced by surface runoff was collected in the sediment ditches. The soil in the ditch was taken out and dried in the air, then weighed. Water content of the air dried soil was measured in air oven at 110°C.

Physical properties of soils

Cylinder intake rate, soil hardness using Yamanaka's cone type penetrometer, bulk density, saturated conductivity, organic matter content using Walkley's method, dispersion ratio and particle size distribution were determined. The results are shown in Table 1. The particle size accumulation curves of both soils are shown in Fig. 2. The accumulation curve indicated a relatively large amount of stable aggregates in the volcanic ash soil, because the clay content shown in Fig. 2, was approximately 18%, a value clearly lower than 50% in the case of complete dispersion determination.

Table 1 Physics of properties of soils in lysimeters on slopes.

	Bulk density (g/cm^3)	Cylinder intake rate (mm/hr)	Saturated conductivity (mm/hr)	Soil 15% slope (kg/cm^2)	Hardness 5% slope (kg/cm^2)	Organic matter content (%)	Dispersion ratio (%)
Sandy soil	1.36	43.0	194.0	4.44	1.48	-	-
Volcanic ash soil	0.63	858.1	192.0	2.96	1.85	1.85	34.8

1) Bulk density values were the average values of five 100 cm^3 samples for each slope of 5 degrees and 15 degrees.
2) Cylinder intake rates were the average values obtained in two points on each slope of 5 degrees.
3) Hydraulic conductivity values were the average values of four 100 cm^3 samples in slope of 7 degrees.
4) Soil hardness values obtained by Yamanaka type hardness meter, were the average values recorded in twelve points on each slope.
5) Organic matter contents and dispersion ratios were the average values of four samples and two samples in each slope of 7 and 15 degrees, respectively.

HYDRAULIC TRANSPORT EQUATION

Dimensionless tractive force and dimensionless sediment transport

Dimensionless expressions of tractive force τ^* and sediment transport q^* are given in equation (1) and equation(2) as proposed by Kalinske (Rouse, 1949).

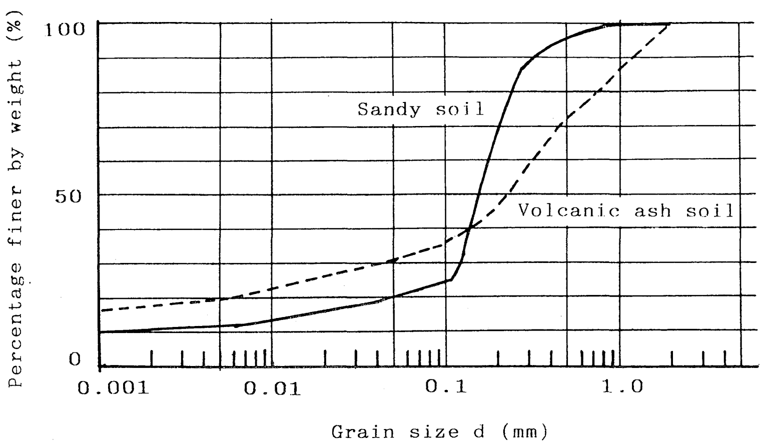

Fig. 2 Grain size accumulation curves in sandy and volcanic ash soils.

$$\tau^* = U^{*2}/(s \cdot g \cdot d) \tag{1}$$

where $U^* = \sqrt{g \cdot h \cdot \sin\Theta}$ is the friction velocity, g is the acceleration due to gravity, h is the water depth, $s = (\sigma - \rho)/\sigma$ is the soil particle density in water, σ and ρ are the densities of soil particles and water, and d is the mean diameter of the soil particles.

$$q^* = qb/(U^* \cdot d) \tag{2}$$

where qb is the weight of the transported sediment per unit time and unit width.

The rain water flow on the soil surface is presumably not uniform due to the very shallow depth and raindrop splash. However since in the current analysis the rain water flow is assumed to be uniform, the tractive force and sediment transport q^* were combined in a power function (equation(3), which applies to a uniform flow (Iwagaki & Tsuchiya, 1957):

$$q^* = A\tau^{*B} \tag{3}$$

where A and B are constants.

Surface runoff and rate of sediment transport

Based in the kinematic wave model, surface runoff caused by rainfalls is expressed by the following equations.

$$h = Kq^P, \ \partial h/\partial t + \partial q/\partial x = re \tag{4}$$

where q is the surface water flow rate per unit width, re is the inflow rate from rainfall, t is time, x is the distance from the upper end, and K and a function of P are expressed as $K = (N/\sqrt{\sin\Theta})^P$ using Manning's equation, where $P = 0.6$, N is the roughness of the surface and Θ is the slope angle.

Substituting equation (3) for equations (1) and (2), the following equations are obtained:

$$qb/(U^{*}d) = A[U^{*2}/(s\cdot g\cdot d)]^{B} \tag{5}$$

$$qb = A(h\cdot \sin\Theta)^{B+0.5}\cdot g^{0.5}\cdot s^{-B}\cdot d^{1-B} \tag{6}$$

"h" in equation (6) is substituted by the motion equation of equation (4) and equation (6) is expressed as equation (7):

$$qb = A\cdot(K\cdot q^{P}\sin\Theta)^{B+0.5}\cdot g^{0.5}\cdot s^{-B}\cdot d^{1-B} \tag{7}$$

By applying Manning's equation the next equation is obtained:

$$qb = A\cdot N^{P(B+0.5)}\cdot \sin\Theta^{(1-0.5P)(B+0.5)}\cdot q^{P(B+0.5)}\cdot s^{-B}\cdot d^{1-B}\cdot g^{.5} \tag{8}$$

When the surface water flow is not measured, the inflow rate *re* from rainfall is substituted for equation (4) and q can be calculated by the method of characteristic curves. Moreover, when a linear relationship is assumed for $q = rm\cdot L$ (rm: average effective rainfall intensity, L: the slope length), equation (8) can be calculated without applying the method of characteristic curves.

Using equation (8), the rate of sediment transport can be estimated at the initial stage of soil erosion in farmland where rill erosion has not yet developed.

RESULTS

Runoff and sediment transport under natural rainfall

The sediment transported by natural rainfall was collected from May to October in 1989. Total rainfall during this period amounted to 1002 mm. Rainfall that caused sediment transport was produced sixty four times including eight experiments using the rain simulator. The values of surface runoff and sediment transport occurred each time was divided by the duration of each surface runoff in order to obtain the flow rate and the rate of transport, and then these rates were converted into dimensionless values. The duration of surface runoff was measured from the runoff records as illustrated in Fig. 3. The range expressed by an arrow mark in the recording paper indicated the duration of high surface flow. As the speed of recording paper was slow, the reading was performed at 15 minute intervals.

Rain simulator experiments

Eight experiments using the rain simulator were carried out on the sloping lysimeters with angles of 7° and 15° filled with sandy soil and volcanic ash soil. Rainfall intensity of the rain simulator remained at constant during the experiment. Rainfall intensities, surface runoff rates and their duration are shown in Table 2.

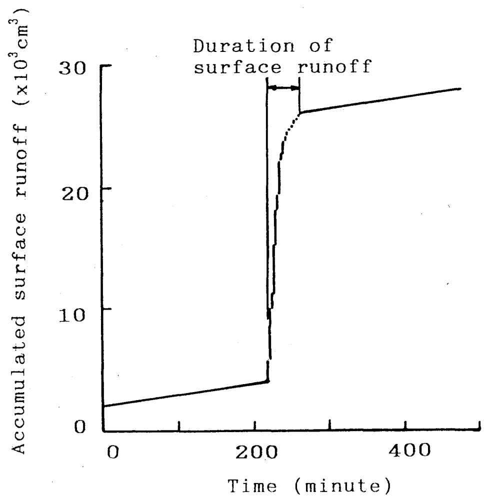

Fig. 3 Method for calculating the duration of surface runoff.

Critical rainfall intensity for surface runoff occurrence

Maximum natural rainfall intensities and surface runoff rates when soil erosion occurred are shown in Table 3. It appeared that the critical rainfall intensity for minimum runoff occurrence was above 7 mm/h. This value was considerably lower than those of the saturated hydraulic conductivities and the cylinder intake rates, presumably due to the formation of a surface crust caused by the raindrop impact, soil detachment and sediments on the bare soil.

RESULTS OF ANALYSIS

Critical tractive force for sediment mixture

Sediments from the slopes of sandy soil and from the volcanic ash soil consisted of a mixture of various particles. The critical tractive force equation of the sediment mixture (Egiazaroff, 1965 and Tsuchiya, 1963) is complex and cannot be applied easily. Therefore the mean diameter of the sediment particles of both soils for the application of the simple equation of critical tractive force for uniform sediment particles, was calculated by the following equation:

$$dm = \Sigma d\Delta p / \Sigma \Delta p \qquad (9)$$

where Δp is the fraction of diameter d. As a result, the mean diameter was 0.019 cm for the sandy soil and 0.032 cm for the volcanic ash soil.

Critical tractive forces τc for uniform sediment particles were calculated according to Iwagaki's equation (Iwagaki, 1956):

$$Uc^{*2} = (0.1235 s \cdot g)^{25/32} \cdot \mu^{7/16} \cdot d^{11/32} \quad 2.14 \leq R^* \leq 54.2 \qquad (10)$$

Table 2 Experimental data under artificial rain.

Soil and slope	Duration of rain (min.)	Rain intensity (mm/hr)	Surface runoff (mm/hr)	Duration of surface runoff (min.)	Erosion (g/m/min.)	Flow velocity (cm/s)	Water depth (mm)
Bare sandy soil, 7°	150	78.2	33.9	136	0.576	35.0	1.95
	150	40.0	18.9	137	0.196	40.1	1.35
Bare volcanic ash soil, 7°	150	78.2	27.0	146	0.272	16.0	1.65
	150	40.0	10.8	135	0.076	17.9	0.95
Bare sandy soil, 15°	120	22.1	2.2	56	0.026	-	-
	70	37.7	22.5	29	0.616	-	-
	40	39.0	23.2	35	0.624	-	-
	40	49.0	27.0	30	0.828	-	-

Table 3 Surface runoff and maximum rainfall intensity for a period of 15 min (expressed as mm per hour).

Date	Time	Rain intensity (mm/h)	Surface runoff (mm/h): Sandy soil with slope: 15°	10°	7°	5°	Volcanic ash soil with slope: 15°	10°	7°	5°
5.26	14:00	14.8	8.6	4.2	4.2	6.1	0.3	6.1	1.9	5.1
5.28	20:00	22.0	3.2	0.0	1.6	3.2	0.0	5.1	0.3	0.0
6.17	0:30	7.2	0.6	0.0	0.3	0.0	0.0	0.0	0.0	0.0
6.24	18:45	7.2	2.6	0.3	0.3	0.3	0.3	0.0	0.0	0.2
7.13	6:45	19.2	6.1	1.3	0.0	1.0	0.3	0.0	0.0	0.0
8.1	2:30	48.0	29.4	29.8	25.9	26.2	1.0	0.0	1.6	1.9
8.6	11:30	22.0	9.0	10.2	6.1	7.7	0.3	4.5	0.3	2.9
8.27	15:30	31.2	16.0	16.0	20.2	25.0	6.7	6.7	3.8	6.7
9.5	15:30	30.0	12.5	9.3	11.2	10.6	7.7	1.9	2.9	5.8
9.20	5:00	36.0	21.4	23.0	23.4	20.2	7.7	7.0	10.9	12.8
9.22	7:45	11.2	1.3	0.0	0.0	0.0	0.0	0.0	0.0	0.0
10.4	8:30	9.2	-	-	0.0	0.0	0.9	0.0	0.0	0.0
10.11	18:15	8.4	-	-	0.0	0.0	1.3	0.0	0.0	0.0
10.19	20:15	17.2	-	-	2.5	4.2	1.9	0.0	0.0	0.0

(-) indicates the absence of measurement.

where Uc^* is the critical friction velocity, μ is the coefficient of kinematic viscosity 0.01 cm^2/s, $g = 980$ cm/s^2, and $R^* = (s \cdot g)^{1/2} \cdot d^{3/2}/\mu$

$$Uc^{*2} = 8.56d^{11/32} \quad 0.0065 \leq d \leq 0.0568, s = 1.7 \text{ (sandy soil)} \quad (11)$$

$$Uc^{*2} = 8.41d^{11/32} \quad 0.0065 \leq d \leq 0.0565, \quad s = 1.65 \text{ (volcanic ash soil)} \quad (12)$$

$$\tau c = Uc^{*2}/(s \cdot g \cdot d) \quad (13)$$

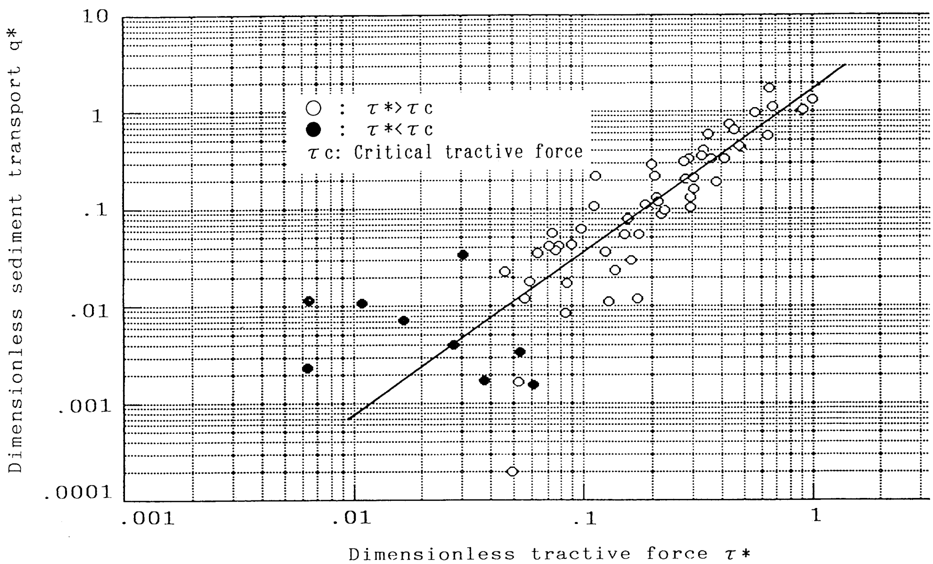

Fig. 4 Dimensionless tractive force vs. dimensionless sediment transport.

=0.0692 cm for the sandy soil, and =0.0498 for the volcanic ash soil.

Dimensionless tractive force and dimensionless sediment transport

As the relationship between the dimensionless tractive force and sediment transport shown in Fig. 4 on a log-log scale fitted a linear regression, the application of equation (3) to the rain water flow was considered to be suitable. The expression of this relation in one regression line regardless of the soil types, was ascribed to the fact that the aggregates of the volcanic ash soil in the surface layer had far broken into smaller aggregates by rain and wind for several years, and the aggregate size became similar to that of sandy soil.

Although the rain water flow contained soil particles detached from the soil surface due to the rain drops, most of the sediment transport was caused by the tractive force of water flow. The effect of splash transport by rain drops appeared to be a little.

Data shown in Fig. 4 were obtained all the experiments using lysimeters on four different slopes filled with two different types of soils. The power regression curve of these dots was:

$$q^* = 1.501\tau^{*1.655} \qquad r = 0.887 \tag{14}$$

where r is a correlation coefficient.

When the value of the dimensionless tractive force was less than 0.07 (Fig. 4), the deviation between the dots and the regression line increased, presumably due to the decrease in the dimensionless tractive force which was lower than the critical tractive force calculated in equation (13).

Simulation of sediment transport using a hydrological erosion model

Coefficients A and B in equation (8) were determined by equation (14). The values of P and g were 0.6 and 980 cm/s^2. The roughness N was calculated by introducing the average water depth and the surface water flow into Manning's equation. The water depth was very low, about 1 mm. In the calculation, values of N = 0.0211 (s/cm$^{1/3}$:sandy soil) and 0.0218 (volcanic ash soil) were used as roughness values. The following equation of qb (g/s/cm) was obtained with $\sin\Theta$ and q (cm^3/s/cm) as variables:

$$qb = \alpha \cdot \sin\Theta^{1.508} \cdot q^{1.293} \tag{15}$$

where, α = 1.785 (sandy soil), and α = 1.386 (volcanic ash soil).

Surface water flow and sediment transport in four kinds of slopes with different gradients

The values of the sediment transport estimated by the equation and the observed data of sediment transport in each slope are shown in Figs 5, 6, 7 and 8. In the figures, the unit of slope width was expressed in meters and the dimensions of q and qb were expressed as cm^3/s/m and g/s/m, respectively.

It was considered that the linear regression obtained by equation (15) fitted well the experimental data and that the data of the two soils could not be separated as the regression lines estimated for both soils were very close.

In Figs 5 and 7 the data obtained by the rain simulator were included and no

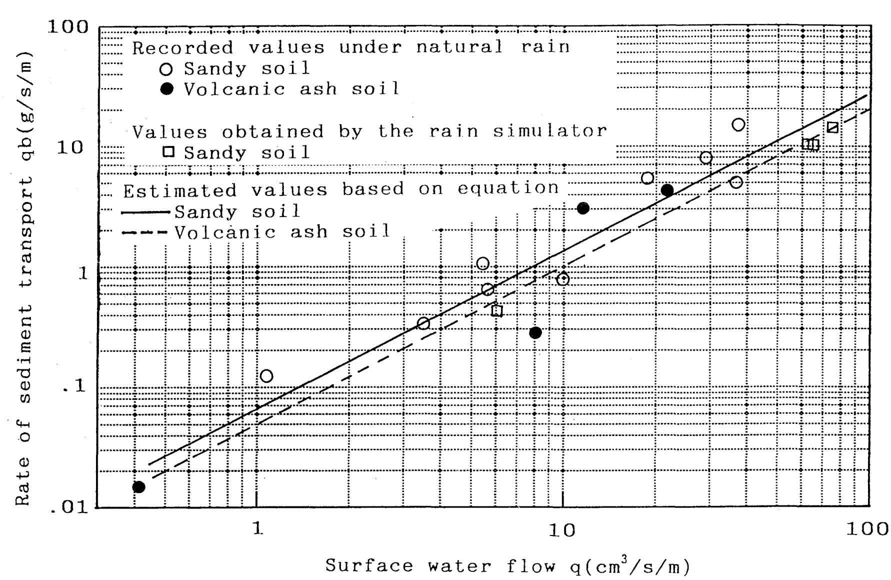

Fig. 5 Recorded values and estimated lines in 15° slopes.

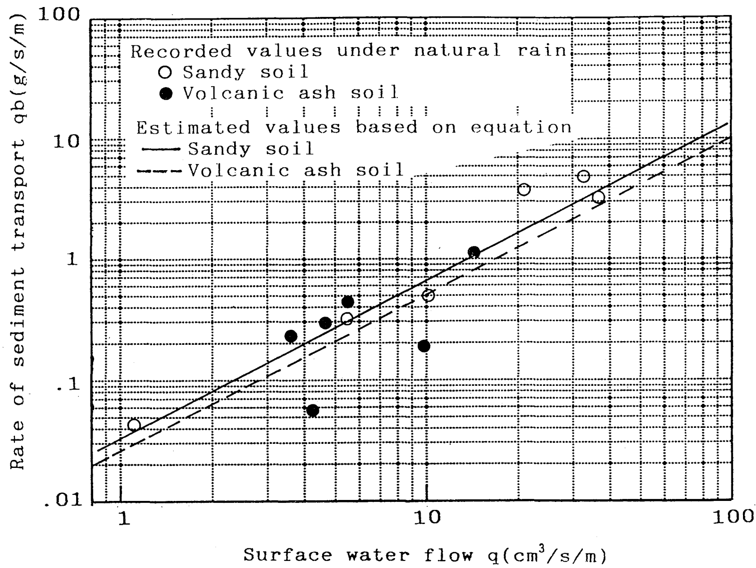

Fig. 6 Recorded values and estimated lines in 10° slopes.

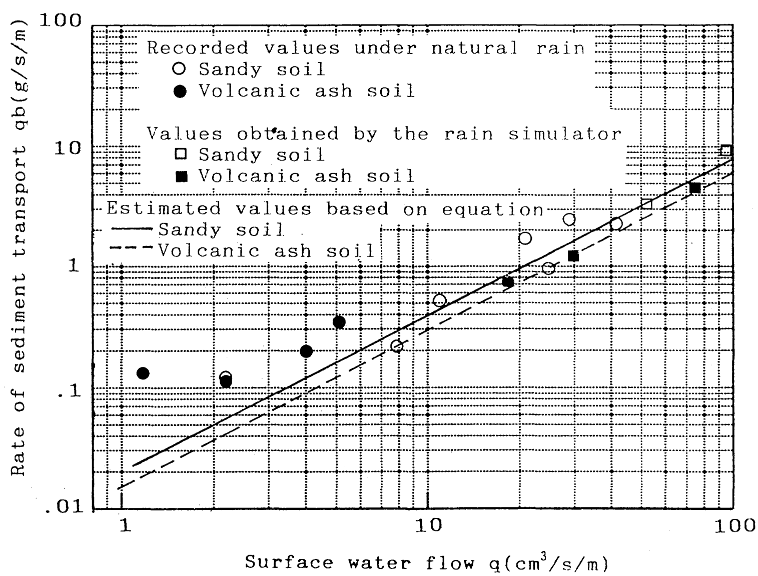

Fig. 7 Recorded values and estimated lines in 7° slopes.

significant difference between natural rain and simulated rains was recognized. Therefore it is suggested that the rain simulator may be suitable for estimating sediment transport under heavy rain that seldom occurs under natural conditions.

In Fig. 7 four values in volcanic ash soil obtained under low water flow conditions under natural rainfall did not fit the equation. In Fig. 8 the estimation of the values in the regression line of sandy soil slightly exceeded the experimental values.

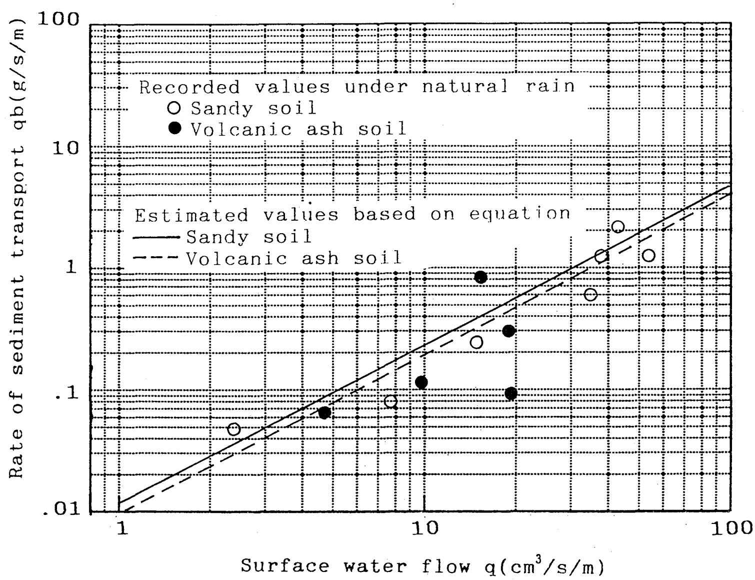

Fig. 8 Recorded values and estimated lines in 5° slopes.

When the water flow was sufficient, the estimation fitted well the experimental data. However, when the water flow was low and the slope gentle, the application of the sediment transport equation was limited due to the effect of the critical tractive force.

Acknowledgements The authors thank K. Shibuya and H. Kamimura for the construction of the lysimeters and the setup of measurements, and N. Horikawa for the assistance in the experiments.

REFERENCES

Banzai, K., Miyazaki, T. & Harakawa, T. (1988) The experimental Study of the erosion from the slope of volcanic ash soil and sand. *Proc. of 5th Int. Soil Conservation Conf.* (Bangkok, Thailand, Jan. 1988), 541-554.

Egiazaroff, I. V. (1965) Calculation of nonuniform sediment concentrations. *J. Hydraul. Div. ASCE* **91**(HY4), 225-247.

Finkner, S. C., Nearing, M. A., Foster, G. R. & Gilley, J. E. (1989) A simplified equation for modeling sediment transport capacity. *Trans. Am. Soc. Agric. Engrs* **32**(5), 1545-1550.

Iwagaki, Y. (1956) Hydrodynamical study on critical tractive force. *Trans. Japan Soc. Civil Engineers, Tokyo, Japan* **41**, 1-21 (in Japanese).

Iwagaki, Y. & Tsuchiya, Y. (1957) On the detachment and the transportation of soil by rain water flow. *Trans. Japan Soc. Civil Engineers, Tokyo, Japan* **51**, 34-40 (in Japanese).

Kilinic, M. Y. (1972) Mechanics of soil erosion from overland flow generated by simulated rainfall. PhD thesis Colorado State Univ., Fort Collins, Colorado, USA.

Komura, S. (1976) Hydraulics of slope erosion by overland flow. *J. Hydraul. Div. ASCE* **102**(HY10), 1573-1586.

Rouse, H. (1949) *Engineering Hydraulics*. John Wiley, New York, USA. 798-799.

Tsuchiya, Y. (1963) Study on the critical tractive force of graded sand gravels, *Annual Report of Disaster Prevention Research Institute, Kyoto Univ., Kyoto, Japan*, **6**, 228-253 (in Japanese).

Yalin, M. S. (1963) An expression for bed-load transportation. *J. Hydraul. Div. ASCE* **89**(HY3), 221-250.